Title

Quadrature Filter Approximation for Reconstructing the Complex Envelope of a Bandpass Signal Sampled Directly With a Two-Channel TIADC

Journal

IEEE Transactions on Circuits & Systems II Express Briefs, 69(6)

ISSN

1549-7747

Authors

Wahab, Mansoor
Levy, Bernard C

Publication Date

2022-06-01

DOI

10.1109/tcsii.2022.3167426

Peer reviewed

Quadrature Filter Approximation for Reconstructing the Complex Envelope of a Bandpass Signal Sampled Directly with a Two-Channel TIADC

Mansoor Wahab, *Student Member, IEEE,* and Bernard C. Levy, *Life Fellow, IEEE*

***Abstract*—A general and flexible technique is proposed for sampling the complex envelope of a bandpass signal by using a nonuniformly interleaved two-channel analog-to-digital converter (TIADC). The signal is sampled directly without any demodulation operation, but the two sampling channels are not uniformly interleaved, since some TIADC timing offsets are rendered forbidden. The proposed complex envelope sampling scheme requires the implementation of two digital FIR filters and a discrete-time modulator. Quadrature sampling, a special case that assumes certain parameter relations, is investigated as an approximation technique. Computer simulations are presented and illustrate a -57dB mean-square error (MSE) can be achieved via quadrature approximation for sufficiently large filter orders.**

***Index Terms*—Bandpass sampling, direct sampling, quadrature sampling, software defined radio, time interleaved A/D converter.**

I. Introduction

Due to their lower hardware complexity, direct bandpass sampling front ends have become attractive for software defined radio and radar applications. However, the implementation of flexible high-resolution bandpass sampling systems presents some challenges. Wide bandwidth sample and hold (S/H) circuits [1] are required for sampling signals located in high frequency bands. Moreover, if a single ADC is used, and B represents the occupied bandwidth of the signal of interest (which differs from its maximum frequency), alias-free reconstruction of the bandpass signal is not guaranteed for all sampling frequencies Ω_s above the Nyquist frequency $2B$ [2], [3], [4, Sec. 6.4]. In addition to being greater than $2B$, Ω_s needs to satisfy certain conditions which depend on the location of the frequency band occupied by the bandpass signal. This creates a significant challenge for software defined radio receivers since different sampling frequencies need to be selected for signals in different bands, even if they have the same bandwidth. To overcome this additional constraint, Kohlenberg proposed second-order sampling, i.e. time-interleaved sampling, where two separate ADCs operating with a time skew sample the signal with frequency $\Omega_s' = \Omega_s/2$. In this case, except for certain forbidden values of the timing offset between the two ADCs, the bandpass signal can be reconstructed from the two time-interleaved sample sequences for all Ω_s above $2B$. This result was extended later by Coulson and others [5], [6] to the case where M time-interleaved ADCs operating at Ω_s/M are used to sample the bandpass signal.

A special case of Kohlenberg's second-order bandpass sampling called quadrature sampling was first proposed by Grace and Pitt [7] and later investigated in detail by Brown [8], [9]. The sub-ADC sampling rate is chosen as an integer fraction of the carrier frequency, while the timing offset is equal to a quarter of the carrier period plus possibly an integer multiple of the carrier period. Quadrature sampling is highly appealing since the data sequences generated by the sub-ADCs are the sampled in-phase and quadrature (I and Q) signal components, i.e., the sampled complex envelope of the signal.

Removed the last sentence in this paragraph due to inaccuracy pointed out by Reviewer 1

In this brief we consider the computation of the sampled complex envelope of a bandpass signal from the sequences produced by a two-channel time-interleaved ADC (TIADC) with timing offset dT_s', where $0 < d < 1$ and $T_s' = 2\pi/\Omega_s'$ denotes the sub-ADC sampling period. Unlike the sub-sampling ADC architecture [10], RF Bandpass $\Delta\Sigma$ ADC [11], and spectral alias spreading [12] technique that all tie the sampling rate to the carrier frequency, our method only requires the sampling frequency Ω_s to be above $2B$. Furthermore, no assumption is made about the carrier frequency Ω_c, signal bandwidth B, sampling frequency Ω_s and timing skew d, except that $\Omega_c > B/2$, which ensures that the signal considered is a bandpass signal. It is shown that the evaluation of the sampled complex envelope requires the implementation of two FIR filters and a digital modulator. Certain timing skews are forbidden, and a precise characterization of these forbidden skews is provided. Reconstruction filters in the case of quadrature sampling are shown to have easy forms and are used in the estimation of the complex envelope when the carrier frequency is not exactly an integer multiple of the sub-ADC sampling rate as required for quadrature sampling.

Comparison with other methods added as suggested by Reviewer 3. Statements restructured.

The brief is organized as follows. The sampling model is described in Section II. This model is used in Section III to compute the sampled complex envelope. Section IV presents sampling and reconstruction for quadrature sampling. Simulations assessing the performance of envelope reconstruction via quadrature approximation are illustrated in Section V. Finally, Section VI provides concluding remarks.

II. Complex envelope sampling model

Consider the bandpass signal

$$\begin{aligned} x_c(t) &= a_c(t)\cos(\Omega_c t) - b_c(t)\sin(\Omega_c t) \\ &= \Re[c_c(t)e^{j\Omega_c t}] = |c_c(t)|\cos(\Omega_c t + \angle c_c(t)) \,, \end{aligned} \quad (1)$$

Bernard C. Levy and and Mansoor Wahab are with the Department of Electrical and Computer Engineering, 1 Shields Avenue, University of California, Davis, CA 95616 (emails: bclevy, mswahab@ucdavis.edu).

where

$$c_c(t) = a_c(t) + jb_c(t) \tag{2}$$

denotes the complex envelope of $x_c(t)$ and the in-phase and quadrature components $a_c(t)$ and $b_c(t)$ are baseband signals with bandwidth $B/2$. If the carrier frequency $\Omega_c > B/2$ (it is in general much larger), the Fourier spectrum $X_c(j\Omega)$ of $x_c(t)$ is contained in two disjoint positive and negative frequency bands $[\Omega_L, \Omega_H]$ and $[-\Omega_H, -\Omega_L]$ with $\Omega_L = \Omega_c - B/2$ and $\Omega_H = \Omega_c + B/2$, so that the occupied bandwidth of $x_c(t)$ is $\Omega_H - \Omega_L = B$. Unlike conventional heterodyne radar or communications receivers [13] which convert $x_c(t)$ to a lower IF frequency, and correlate it with two quadrature IF oscillators to obtain the sampled in-phase and quadrature components, we consider here a direct bandpass sampling receiver where two time-interleaved ADCs sample $x_c(t)$ as shown in Fig. 1.

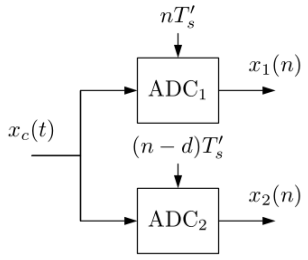

Fig. 1. Time-interleaved sampling of bandpass signal $x_c(t)$.

T_s' denotes the sampling period of the sub-ADCs, which have therefore sampling frequency $\Omega_s' = 2\pi/T_s' = \Omega_s/2$, where Ω_s denotes the sampling frequency of the overall ADC. It is assumed that $\Omega_s > 2B$, or equivalently $\Omega_s' > B$. The timing offset between the two ADCs is $D = dT_s'$ with timing skew $0 < d < 1$. For $d = 1/2$, the combination of the two sub-ADCs forms a uniform ADC with sampling period $T_s = T_s'/2$, but for $d \neq 1/2$, the overall ADC has a nonuniform but periodic sampling pattern. Note also that the use of a timing skew $d \neq 1/2$ implies that that the sub-ADCs cannot share the same S/H. Finally, it is assumed that both channels are matched in terms of gain and bandwidth and that there is no timing skew mismatch.

Let

$$\ell = \text{round}\big(\frac{\Omega_c}{\Omega_s'}\big)\,, \tag{3}$$

so that Ω_c belongs to the frequency band $[(\ell - 1/2)\Omega_s', (\ell + 1/2)\Omega_s']$. Since this frequency band corresponds to the location of the ℓ-th image copy of a sampled baseband signal, it is referred to here as the ℓ-th image band. In the following it is assumed that $\ell \geq 1$, so that the signal $x_c(t)$ is a bandpass signal. If we consider the discrete modulation frequency

$$\omega_b = \Omega_c T_s' \bmod 2\pi = \Big(\frac{\Omega_c}{\Omega_s'} - \ell\Big)2\pi\,, \tag{4}$$

so that $-\pi < \omega_b \leq \pi$, the sampled sequence $x_1(n)$ can be expressed as

$$x_1(n) = x_c(nT_s') = \Re\{c(n)e^{j\omega_b n}\} \tag{5}$$

where $c(n) = c_c(nT_s')$ denotes the sampled complex envelope. Similarly by observing that

$$e^{j(n-d)\Omega_c T_s'} = e^{j(n-d)(\omega_b + 2\pi\ell)} = e^{j\omega_b(n-d)}e^{-j2\pi\ell d}$$

we can express the sampled sequence $x_2(n)$ as

$$x_2(n) = x_c((n-d)T_s') = \Re\{c(n-d)e^{j\omega_b(n-d)}e^{-j2\pi\ell d}\}. \tag{6}$$

In this expression $c(n-d)$ is a shorthand notation for

$$c(n-d) = f(n) * c(n) \tag{7}$$

where $*$ represents the discrete convolution operation and

$$f(n) = \frac{\sin(\pi(n-d))}{\pi(n-d)} \tag{8}$$

is the impulse response of the periodic fractional delay filter which can generally be expressed as

$$F(e^{j\omega}) = e^{-j(\omega - q(\omega))d} \tag{9}$$

for all ω, where

$$q(\omega) = k2\pi \quad \text{for} \quad (2k-1)\pi \leq \omega < (2k+1)\pi$$

represents the quantized value of ω produced by an infinite quantizer with step size 2π.

The Fourier transform of sequence

$$s(n) = c(n-d)e^{j\omega_b(n-d)}e^{-j2\pi\ell d} \tag{10}$$

appearing in (6) is given by

$$\begin{aligned} S(e^{j\omega}) &= F(e^{j(\omega-\omega_b)})C(e^{j(\omega-\omega_b)})e^{-j(\omega_b+2\pi\ell)d} \\ &= F(e^{j\omega})G(e^{j\omega})C(e^{j(\omega-\omega_b)})\,, \end{aligned} \tag{11}$$

where

$$C(e^{j\omega}) = \sum_{n=-\infty}^{\infty} c(n)e^{-j\omega n} \tag{12}$$

denotes the discrete-time Fourier transform (DTFT) of $c(n)$ and the filter

$$\begin{aligned} G(e^{j\omega}) &\triangleq \frac{F(e^{j(\omega-\omega_b)})}{F(e^{j\omega})}e^{-j(\omega_b+2\pi\ell)d} \\ &= e^{-j(q(\omega)-q(\omega-\omega_b))d}e^{-j2\pi\ell d} \end{aligned} \tag{13}$$

is a piecewise constant frequency dependent phase shift. For $\omega_b > 0$, it can be expressed as

$$G(e^{j\omega}) = \begin{cases} e^{-j2\pi(\ell+1)d} & -\pi \leq \omega < -\pi + \omega_b \\ e^{-j2\pi\ell d} & -\pi + \omega_b \leq \omega < \pi\,, \end{cases} \tag{14}$$

and for $\omega_b < 0$, we have

$$G(e^{j\omega}) = \begin{cases} e^{-j2\pi\ell d} & -\pi \leq \omega \leq \pi + \omega_b \\ e^{-j2\pi(\ell-1)d} & \pi + \omega_b < \omega < \pi\,. \end{cases} \tag{15}$$

Since the impulse response $f(n)$ of fractional delay filter $F(e^{j\omega})$ is real, the discrete-time model (5)–(6) can be represented in block diagram form as shown in Fig. 2. In this model, $F(e^{j\omega})$ describes the relative timing skew between the two sub-ADCs, whereas the filter $G(e^{j\omega})$ depends on the image band index ℓ of Ω_c and its relative location ω_b within this band. Thus, from a software defined radio perspective, $G(e^{j\omega})$ changes if the frequency band of the signal of interest varies, but $F(e^{j\omega})$ stays the same.

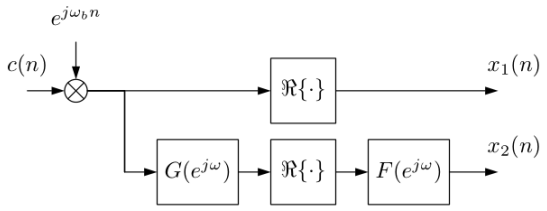

Fig. 2. Discrete-time bandpass sampling model

III. Complex envelope computation

We consider the problem of recovering $c(n)$ from $x_1(n)$ and $x_2(n)$. Note first that since $c(n)$ is complex, $C(e^{j\omega})$ is devoid of symmetries, so knowledge of $C(e^{j\omega})$ over the entire frequency band $[-\pi, \pi]$ is needed to recover $c(n)$. The DTFTs of $x_1(n)$ and $x_2(n)$ are given by

$$X_1(e^{j\omega}) = \frac{1}{2}[C(e^{j(\omega-\omega_b)}) + C^*(e^{-j(\omega+\omega_b)})] \tag{16}$$

and

$$\begin{aligned} X_2(e^{j\omega}) &= \frac{F(e^{j\omega})}{2}[G(e^{j\omega})C(e^{j(\omega-\omega_b)}) \\ &\quad +G^*(e^{-j\omega})C^*(e^{-j(\omega+\omega_b)})]\,. \end{aligned} \tag{17}$$

In each of these expressions, the superposition of $C(e^{j(\omega-\omega_b)})$ and $C^*(e^{-j(\omega+\omega_b)})$ makes it impossible to recover each of these functions separately from either $X_1(e^{j\omega})$ or $X_2(e^{j\omega})$ alone. But (16) and (17) can be written together in matrix form as

$$\begin{bmatrix} X_1(e^{j\omega}) \\ F^{-1}(e^{j\omega})X_2(e^{j\omega}) \end{bmatrix} = \mathbf{M}(e^{j\omega}) \begin{bmatrix} C(e^{j(\omega-\omega_b)}) \\ C^*(e^{-j(\omega+\omega_b)}) \end{bmatrix}, \tag{18}$$

where the matrix

$$\mathbf{M}(e^{j\omega}) = \frac{1}{2}\begin{bmatrix} 1 & 1 \\ G(e^{j\omega}) & G^*(e^{-j\omega}) \end{bmatrix} \tag{19}$$

is invertible as long as its determinant is nonzero. We find

$$D(e^{j\omega}) = \frac{j}{2}\sin(2\pi\ell d)$$

for $0 \le |\omega| \le \pi - |\omega_b|$, and

$$D(e^{j\omega}) = \frac{j}{2}e^{j\pi \mathrm{sgn}(\omega)d}\sin(\pi(2\ell + \mathrm{sgn}(\omega_b))d)$$

for $\pi - |\omega_b| < |\omega| < \pi$, where $\mathrm{sgn}(\omega)$ denotes the sign of ω. Accordingly, the determinant $D(e^{j\omega})$ will be nonzero as long as the timing skew d is such that both $\sin(2\pi\ell d)$ and $\sin(\pi(2\ell + \mathrm{sgn}(\omega_b))d)$ are nonzero. The values

$$d_m^i = \frac{m}{2\ell} \tag{20}$$

with m integer such that $1 \le m \le 2\ell - 1$, and

$$d_q^e = \frac{q}{2\ell + \mathrm{sgn}(\omega_b)} \tag{21}$$

with q integer such that $1 \le q \le 2\ell + \mathrm{sgn}(\omega_b) - 1$, form the *forbidden timing skews*. When $\mathbf{M}(e^{j\omega})$ is invertible for all ω, we obtain

$$C(e^{j(\omega-\omega_b)}) = H_1(e^{j\omega})X_1(e^{j\omega}) + H_2(e^{j\omega})X_2(e^{j\omega}) \tag{22}$$

where the filters

$$\begin{aligned} &\begin{bmatrix} H_1(e^{j\omega}) & H_2(e^{j\omega}) \end{bmatrix} \\ &= \begin{bmatrix} 1 & 0 \end{bmatrix}\mathbf{M}^{-1}(e^{j\omega})\begin{bmatrix} 1 & 0 \\ 0 & F^{-1}(e^{j\omega}) \end{bmatrix} \\ &= \frac{1}{2D(e^{j\omega})}\begin{bmatrix} G^*(e^{-j\omega}) & -F^{-1}(e^{j\omega}) \end{bmatrix}. \end{aligned} \tag{23}$$

Since $C(e^{j(\omega-\omega_b)})$ is the Fourier transform of the modulated signal $r(n) = e^{j\omega_b n}c(n)$, $c(n)$ can be recovered by demodulating $r(n)$, as shown in Fig. 3.

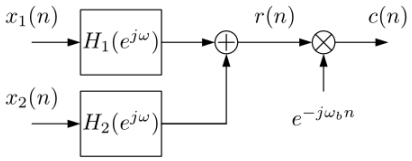

Fig. 3. Recovery of $c(n)$ from $x_1(n)$ and $x_2(n)$

Substituting the expressions for $D(e^{j\omega})$ and $G(e^{j\omega})$ inside (23) gives

$$H_1(e^{j\omega}) = \frac{e^{j2\pi\ell d}}{j\sin(2\pi\ell d)} = 1 - j\cot(2\pi\ell d) \tag{24}$$

for $|\omega| \le \pi - |\omega_b|$ and

$$\begin{aligned} H_1(e^{j\omega}) &= \frac{e^{j\pi(2\ell+\mathrm{sgn}(\omega_b))d}}{j\sin(\pi(2\ell+\mathrm{sgn}(\omega_b))d)} \\ &= 1 - j\cot(\pi(2\ell+\mathrm{sgn}(\omega_b))d) \end{aligned} \tag{25}$$

for $\pi - |\omega_b| < |\omega| \le \pi$. Similarly, we find

$$H_2(e^{j\omega}) = j\frac{e^{j\omega d}}{\sin(2\pi\ell d)} \tag{26}$$

for $|\omega| \le \pi - |\omega_b|$ and

$$H_2(e^{j\omega}) = j\frac{e^{j(\omega-\pi\mathrm{sgn}(\omega))d}}{\sin(\pi(2\ell+\mathrm{sgn}(\omega_b))d)} \tag{27}$$

for $\pi - |\omega_b| < |\omega| < \pi$. The impulse responses of filters H_1 and H_2 can be approximated by causal FIR filters of order $M = 2L$ by shifting the impulse responses by L and applying a Kaiser window of length $M+1$. In this case, the output $\hat{c}(n-L)$ of the reconstruction block diagram is only an estimate of the complex envelope at time $n - L$. With respect to filter complexity, using Fourier Transform symmetry properties it can be observed that each of the complex filters H_1 and H_2 requires only the implementation of a single real FIR filter.

IV. Special Case: Quadrature Sampling

Unlike previously published results on TIADC sampling of the envelope of bandpass signals, our analysis behind the sampling and reconstruction models placed no restrictions on Ω_c, Ω_s, B and d beyond $\Omega_c > \Omega_s'/2 > B/2$ (Ω_c cannot be in the baseband and Ω_s is above the Nyquist rate). Earlier results [7]–[9], [14], [15] typically assume relations between Ω_s and Ω_c and between d and Ω_c. For example, for quadrature sampling as originally defined by Grace and Pitt [7] and further investigated by several authors [8], [9], [16], $\Omega_s' = \Omega_c/\ell$

References slightly restructured

with ℓ integer, so that Ω_c is exactly at the center of the ℓ-th image band resulting in $\omega_b = 0$. Furthermore, the timing offset between the two ADCs is chosen as $D = T_c/4 + pT_c$ with p integer and $T_c = 2\pi/\Omega_c$. This gives

$$d = \frac{D}{T_s'} = \frac{1}{4\ell} + \frac{p}{\ell} \tag{28}$$

so $2\pi\ell d = \pi/2 + 2\pi p$. In this case equations (5) and (6) reduce to

$$\begin{aligned} x_1(n) &= a(n) = a_c(nT_s') \\ x_2(n) &= b(n-d) = b_c((n-d)T_s') \,, \end{aligned}$$

so that the two sub-ADCs sample independently the in-phase and quadrature components of the bandpass signal. The phase-shifting filter in (14–15) reduces to $G(e^{j\omega}) = -j$, and the determinant of matrix $\mathbf{M}(e^{j\omega})$ becomes $D(e^{j\omega}) = j/2$ which is nonzero for all $\omega \in [-\pi, \pi]$ indicating the timing skew (28) is not forbidden. Reconstruction filters simplify to

$$H_1(e^{j\omega}) = 1, \;\; H_2(e^{j\omega}) = je^{j\omega d}, \tag{29}$$

with respective impulse responses

$$h_1(n) = \delta(n), \;\; h_2(n) = j\,\frac{\sin[\pi(n+d)]}{\pi(n+d)} \,. \tag{30}$$

From a practical standpoint, reconstruction is greatly simplified since only a non-integer advance filter is required which can be implemented causally with insertion of a delay. In spite of its elegance, quadrature sampling does present challenges. The timing skew d in (28) becomes quite small for signals located in higher image bands imposing strict jitter requirements for the sampling clocks and necessitating TIADC calibration. Moreover, the carrier frequency of the received signal may not be exactly an integer multiple of the sub-ADC sampling rate. This motivates assessing envelope reconstruction in the presence of carrier frequency deviations away from its ideal value. Let $\Omega_c^0 = \ell\Omega_s'$ be the theoretical carrier frequency desired and

Mention of calibration added. Sentence revised.

$$\Omega_c = \Omega_c^0 + \varepsilon \tag{31}$$

the actual signal carrier frequency at the receiver. The frequency offset technically satisfies $|\varepsilon| < \Omega_s'/2$, but in practice will be much smaller. Evaluating (4) using (31) gives $\omega_b = \varepsilon T_s'$, so different sequences $x_1(n)$, $x_2(n)$ are generated based on expressions (5–6) as ε varies. Although ω_b is nonzero for all $\varepsilon \neq 0$, the complex envelope can be reconstructed approximately using the quadrature case filters (29) which were computed under the assumption that $\omega_b = 0$. The performance of this method will be analyzed in section V.

V. Simulations

To illustrate the proposed direct complex envelope sampling method, consider a bandpass signal with theoretical carrier frequency $F_c^0 = \Omega_c^0/(2\pi) = 5$GHz, and continuous-time envelope

$$\begin{aligned} c_c(t) &= \frac{3}{2}e^{j400\times10^6\times2\pi t} + \frac{1}{2}e^{-j400\times10^6\times2\pi t} \\ &\quad + \frac{j}{2}[e^{j175\times10^6\times2\pi t} + e^{-j175\times10^6\times2\pi t}] \end{aligned} \tag{32}$$

with bandwidth $(B/2)/(2\pi) = 400$MHz. The choice of sub-ADC sampling frequency $F_s' = \Omega_s'/(2\pi) = 1$GHz is above $B/(2\pi) = 800$MHz, as required by the Nyquist sampling criterion. Since

$$F_c = F_c^0 + \frac{\varepsilon}{2\pi} = 5F_s' + \frac{\varepsilon}{2\pi} \,,$$

and $|\varepsilon|/(2\pi) < F_s'/2$, we have $\ell = 5$, i.e., F_c is located in the 5-th image band. The value of ω_b will vary with different ε, but will be close to zero for ε sufficiently small. The discrete-time envelope obtained by sampling $c_c(t)$ with sampling period $T_s' = 1/F_s'$ is

$$\begin{aligned} c(n) = c_c(nT_s') &= \frac{3}{2}e^{j0.8\pi n} + \frac{1}{2}e^{-j0.8\pi n} \\ &\quad + \frac{j}{2}[e^{j0.35\pi n} + e^{-j0.35\pi n}] \end{aligned} \tag{33}$$

This signal has four tones located at $\pm0.8\pi$ and $\pm0.35\pi$, but the tone at 0.8π has an amplitude three times larger than the tones at -0.8π and $\pm0.35\pi$.

To sample $x_c(t)$, we select a TIADC with nominal timing skew $d_0 = 1/(4\ell) = 0.05$ which is the simplest case of quadrature timing skew from (28). The ADC and FIR filters are simulated in Matlab using floating-point arithmetic. In the simulations two independent white noise sequences modelling the effect of thermal and quantization noises are added to the sub-ADC outputs $x_1(n), x_2(n)$. The sub-ADC SNR is 61.8dB. In the reconstruction block diagram shown in Fig. 3, quadrature reconstruction filters (29) are used as an approximation to the actual filters given in (24–27). The FIR filters $H_1(z)$ and $H_2(z)$ have order $M = 16$ and are obtained by applying a Kaiser window with parameter $\beta = 6$ to the impulse responses $h_1(n)$ and $h_2(n)$ in (30).

New statement added

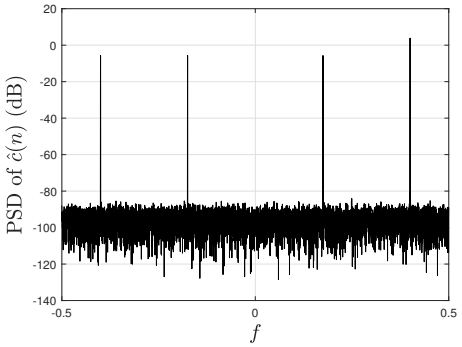

Fig. 4. PSD of the estimated envelope $\hat{c}(n)$ for $\varepsilon = \omega_b = 0$ computed with FIR filters of order $M = 16$ for a TIADC with quadrature timing skew $d_0 = 0.05$.

The PSD of the estimated envelope $\hat{c}(n)$ is plotted in Fig. 4 on domain $-1/2 \leq f \leq 1/2$, where $f = \omega/(2\pi)$, for $\varepsilon = 0$, i.e. $F_c = F_c^0$ and $\omega_b = 0$. It is computed by using the periodogram method with a Kaiser window for a data segment with $N = 10^4$ samples. The periodogram is scaled so that a complex tone with unit amplitude corresponds to 0dB. The estimated envelope has correct positioning and scaling of the four desired tones indicating successful reconstruction. Since the exact envelope $c(n)$ is known, the error $\tilde{c}(n) = c(n) - \hat{c}(n)$ can be evaluated, and the MSE is -50.56dB.

Sentence revised to clarify the domain of Fig. 4

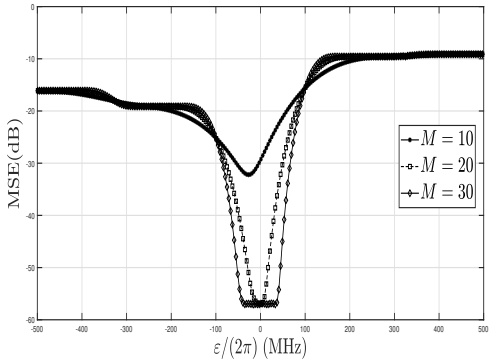

Fig. 5. MSE for the entire range of ε values computed with FIR filters of order $M = 10, 20, 30$ in the case of quadrature timing skew $d_0 = 0.05$.

The MSE is plotted in Fig. 5 for $|\varepsilon|/(2\pi) < F_s'/2 = 500$MHz when different filter orders are used to estimate the envelope. Higher filter orders $M = 20, 30$ offer significant performance gain around $\varepsilon = 0$ in comparison to $M = 10$, but present no advantage beyond $|\varepsilon|/(2\pi) > 100$MHz. In the case of $M = 30$, frequency offsets up to ± 40MHz can be tolerated without any performance loss. In this range $\omega_b \approx 0$, so the filters (24–27) strongly resemble quadrature filters (29) used in envelope estimation. However, implementing filters with length $M + 1 = 31$ can be challenging in practice. It is worth observing the MSE is not symmetric with respect to $\varepsilon = 0$. This asymmetry is due to the fact that for $\omega_b > 0$ the approximation of the dominant tone of $c(n)$ at $+0.8\pi$ is slightly worse than in the case of $\omega_b < 0$. Finally, a plot similar to Fig. 5 can be obtained for the case when the TIADC suffers from mismatches. For example, it can be shown that in the case of 1% gain mismatch and 0.10% timing skew mismatch, the MSE drops by 30dB in the vicinity of $\varepsilon = 0$ for $M = 20, 30$, but only by 7dB when $M = 10$. This indicates TIADC calibration is especially necessary when higher order filters are used in envelope reconstruction.

VI. Conclusions

In this paper we have described a method for computing the sampled complex envelope of a bandpass signal by sampling the signal directly with a two-channel TIADC and using two digital filters. A special case known as quadrature sampling requires the implementation of only one reconstruction filter and can be used to estimate the envelope even when the carrier frequency is not exactly an integer multiple of the sub-ADC sampling frequency. Simulations demonstrated this technique to be a robust and efficient approximation dependent on the order of reconstruction filters. The analysis presented here ignored the effect of TIADC mismatches. Some recent semi-blind [18]–[20] and fully blind [21]–[23] TIADC calibration techniques have been developed for the bandpass signal case, but they would need to be extended to nonuniformly interleaved ADCs before they can be applied here to correct mismatches. The proposed TIADC and reconstruction filter architecture could be implemented as a software radio front end capable of digitizing signals in different bands.

References

[1] S. Daneshgar, Z. Griffith, M. Seo, and M. J. W. Rodwell, "Low distortion 50 GSamples/s track-hold and sample-hold amplifiers," *IEEE J. Solid-State Circuits*, vol. 49, pp. 2114–2126, Oct. 2014.

[2] A. Kohlenberg, "Exact interpolation of band-limited functions," *J. Applied Physics*, vol. 24, pp. 1432–1436, Dec. 1953.

[3] R. G. Vaughan, N. L. Scott, and D. R. White, "The theory of bandpass sampling," *IEEE Trans. Sig. Proc.*, vol. 39, pp. 1973–1984, Sept. 1991.

[4] J. G. Proakis and D. G. Manolakis, *Digital Signal Processing: Principles, Algorithms, and Applications, 4th edition*. Upper Saddle River, NJ: Prentice-Hall, 2007.

[5] A. J. Coulson, "A generalization of nonuniform bandpass sampling," *IEEE Trans. Sig. Proc.*, vol. 41, pp. 694–704, Mar. 1995.

[6] Y.-P. Lin and P. Vaidyanathan, "Periodically nonuniform sampling of bandpass signals," *IEEE Transactions on Circuits and Systems II: Analog and Digital Signal Processing*, vol. 45, no. 3, pp. 340–351, 1998.

[7] O. D. Grace and S. P. Pitt, "Quadrature sampling of high frequency waveforms," *J. Acoust. Soc. Amer.*, vol. 44, pp. 1453–1454, 1968.

[8] J. L. Brown, Jr., "On quadrature sampling of bandpass signals," *IEEE Trans. Aerospace Elec. Syst.*, vol. 15, May 1979.

[9] J. L. Brown, Jr., "A simplified approach to optimum quadrature sampling," *J. Acoust. Soc. Amer.*, vol. 67, pp. 1659–1662, May 1980.

[10] R. Nanda, H. Chen, and D. Marković, "A low-power digital front-end direct-sampling receiver for flexible radios," in *IEEE Asian Solid-State Circuits Conference 2011*, pp. 377–380, 2011.

[11] E. Martens, A. Bourdoux, A. Couvreur, R. Fasthuber, P. Van Wesemael, G. Van der Plas, J. Craninckx, and J. Ryckaert, "RF-to-Baseband digitization in 40 nm CMOS with RF bandpass $\Delta\Sigma$ modulator and polyphase decimation filter," *IEEE Journal of Solid-State Circuits*, vol. 47, no. 4, pp. 990–1002, 2012.

[12] C. Yang, M. Ayesh, A. Zhang, T.-F. Wu, and M. S.-W. Chen, "A 29-mW 26.88-GHz non-uniform sub-sampling receiver front-end enabling spectral alias spreading," in *2020 IEEE Radio Frequency Integrated Circuits Symposium (RFIC)*, pp. 87–90, 2020.

[13] S. Mirabassi and K. Martin, "Classical and modern receiver architectures," *IEEE Communic. Magazine*, Nov. 2000.

[14] Y.-R. Sun and S. Signell, "Generalized bandpass sampling with FIR filtering," in *Proc. 2005 IEEE Internat. Symp. Circuits Systems*, (Kobe, Japan), pp. 4429–4432, May 2005.

[15] Y.-R. Sun, *Generalized bandpass sampling receivers of software defined radio*. PhD thesis, Royal Institute of Technology, Stockholm, Sweden, 2006.

[16] A. G. Dempster, "Quadrature bandpass sampling rules for single- and multiband communications and satellite navigation receivers," *IEEE Trans. Aerospace Elec. Syst.*, vol. 47, Oct. 2011.

[17] A. V. Oppenheim and R. W. Schafer, *Discrete-Time Signal Processing, 3rd edition*. USA: Prentice Hall Press, 2009.

[18] F. Harris, X. Chen, E. Venosa, and F. A. N. Palmieri, "Two-channel TI-ADC for communication signals," in *Proc. 2001 IEEE 12th Internat. Workshop on Signal Proc. Advances in Wireless communications (SPAWC' 11)*, (San Francisco, CA), pp. 576–580, June 2011.

[19] F. J. Harris, "Artifact-corrected time-interleaved ADC." US Patent No. 8,957,798, Feb. 2015.

[20] M. Waltari, "Time-interleaved analog-to-digital converter for signals in any Nyquist zone." US Patent No. 8,654,000, Feb. 2014.

[21] H. L. Duc, C. Jabbour, P. Desgreys, O. Jamin, and N. Van Tam, "A fully digital background calibration of timing skew in undersampling TI-ADC," in *2014 IEEE 12th International New Circuits and Systems Conference (NEWCAS)*, 2014.

[22] H. Le Duc, D. M. Nguyen, C. Jabbour, T. Graba, P. Desgreys, O. Jamin, and V. T. Nguyen, "All-digital calibration of timing skews for TIADCs using the polyphase decomposition," *IEEE Transactions on Circuits and Systems II: Express Briefs*, vol. 63, no. 1, pp. 99–103, 2016.

[23] H. Le Duc, D. M. Nguyen, C. Jabbour, P. Desgreys, O. Jamin, and V. Tam Nguyen, "Fully digital feedforward background calibration of clock skews for sub-sampling TIADCs using the polyphase decomposition," *IEEE Transactions on Circuits and Systems I: Regular Papers*, vol. 64, no. 6, pp. 1515–1528, 2017.

New references added per reviewer recommendation